

Texture and Microstructure Evolution of AA1100 during Accumulative Roll Bonding

Jaehyung Cho¹, Hyung-Wook Kim¹, and Cha-Yong Lim¹

¹Korea Institute of Materials Science

797 Chanwondaero Chanwon, KyungNam, South Korea, 641-831

Accumulative rolling bonding (ARB) process has been known as one of the severe plastic deformation (SPD) processes. In this study, texture and microstructure evolution of AA1100 alloys during ARB was investigated. Three layers of full-annealed AA1100 alloys were stacked and cold-rolled. The ARB process was repeated up to 5 passes (243 layers). Reduction in area was about 67% per pass. HR-EBSD (high-resolution electron backscatter diffraction) with HKL Channel5 was used to observe texture and microstructure evolution. With increase in rolling pass or reduction in area, grain size grew finer and aspect ratio of the grains increased. Initial texture disappeared during rolling, and typical rolling texture of fcc metals, α (Goss-Brass) and β (Brass-S-Copper) fibers increased. In particular, β (Brass-S-Copper) was dominant after 5 passes. Using TEM (transmission electron microscope) and SOS (scalar orientation spread, one of the misorientation measure), variations of dislocation density and microstructure were investigated. After 1st pass, dislocation density was great and dislocation tangle and dislocation cell were found a lot. With increase in reduction in area, subgrain boundaries were formed and high angle grain boundaries developed. After 5th pass, high angle grain boundaries was clear and few dislocations were found inside grains because of enhanced dynamic recovery.

Keywords: *accumulative roll bonding, AA1100, texture, microstructure, EBSD*

1. Introduction

Severe plastic deformation (SPD), such as equal channel angular extrusion (ECAE) or accumulative roll bonding (ARB) for various metals produces ultra-fine grained microstructure and enhances mechanical properties [1-7]. The increase in yield strength (σ_y) is associated with a decrease in grain size, and the well-known Hall-Petch equation is still valid for sub-micron grains down to about 0.2 μm . It has been known that fracture resistance and superplasticity are also increased.

ARB process is a very effective method to produce ultra-fine grained structure. Repetition of several processes of cutting, cleaning, stacking and rolling produced severe strains [4]. Steel, aluminum and magnesium alloys were successfully utilized for the ARB process. In this research, we applied ARB process to commercial composition of AA1100 aluminum alloys. Three layers of the AA1100 sheets were cleaned, stacked and cold-rolled. Microstructure and texture evolution were investigated with ARB passes up to 5. Mechanical properties of ARBed sheets were also examined.

2. Experimental procedure

ARB process was applied to commercial AA1100 alloys. Initial AA1100 plates with a thickness 6 mm were cold-rolled down to 1 mm with an overall reduction in area of 10 percent for each pass. The roll diameter was 175 mm and the rolling speed was about 2.7 mpm (meter per minute). The sheets with a thickness of 1 mm were fully annealed 1 hour at 400°C. The annealed sheets were cut to have a dimension of 100 mm in width and 300 mm in length. Three layers were cleaned and stacked together. About 67 percent reduction in thickness was made for each pass without lubrication. The roll speed was 3 mpm. No heating was made for both samples and rolls. After 5 ARB passes, the total number

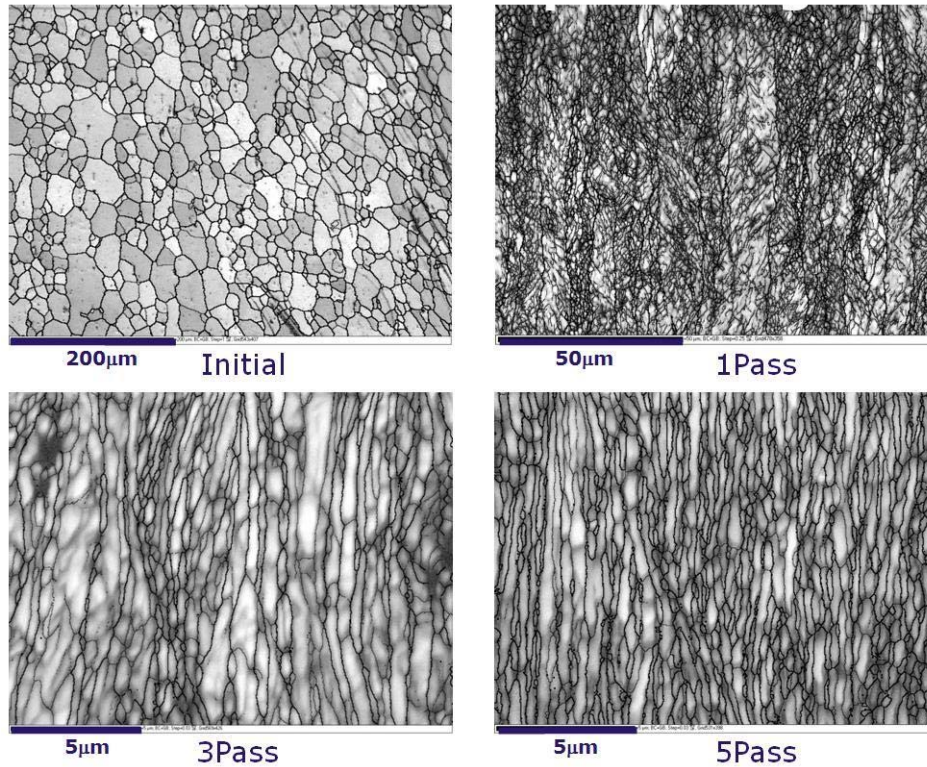


Fig. 1. Kikuchi band contrast maps for ARBed sheets of AA1100. Note that each maps has different magnification and thus different pixel size.
(Thick lines for GID=15°; thin lines for GID =2°)

of layers was 3^5 . Von Mises equivalent strain for each pass was given as, $\varepsilon = \left[\frac{2}{\sqrt{3}} \ln\left(\frac{1}{3}\right) \right] n$, or $\varepsilon = 1.28n$ [8], where n is the number of pass.

Tensile tests at room temperature were carried out using a standard universal testing machine (Instron 4206) at an initial strain rate of $1.67 \cdot 10^{-3}$ /s. The ARB processed sheets were machined to the subsize of the ASTM E8M tensile specimen, whose dimensions were 6 mm in gage width and 25 mm in gage length. The specimens were prepared so that the tensile direction was parallel to the rolling direction (RD) of the sheets.

Microstructure and microtexture were measured along the thickness direction, using a JEOL 7001F FEG-SEM (field emission gun scanning electron microscope) equipped with a HKL Channel5 system. EBSD samples were prepared using an solution of 15ml 2-Butoxyethanol ($C_6H_{14}O_2$) + 85 ml Ethanol (C_2H_6O). Step sizes for EBSD mapping were changing with ARB pass from 1 μm (1 pass) to 0.03 μm (5 passes). More detailed examination of microstructure was made using a JEM-2100F TEM operating at 200 kV. Thin foils for TEM observations were prepared by twin-jet electro-polishing in a 300 ml Nitric acid (HNO_3) + 600 ml Methanol (CH_3OH) solution.

3. Results and discussion

Microstructure and texture were investigated and Fig. 1 shows grain boundary and Kikuchi band contrast maps obtained from EBSD. Initial microstructure of fully-annealed AA1100 sheets displays equi-axed grains. It seems that the first cycle of ARB process developed a lot of substructures. Some

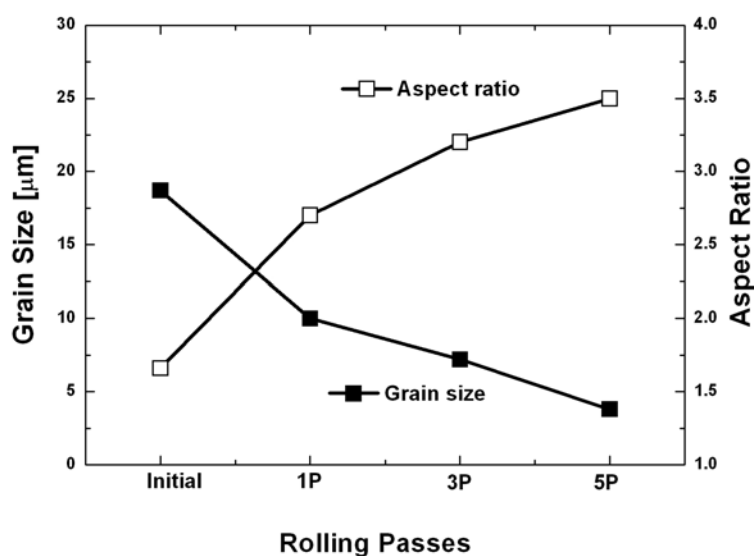


Fig. 2. Variations in grain size and aspect ratio during ARB.

grains elongated along the rolling direction kept their original high angle grain boundaries and contained low misorientation angle inside. Thick lines represent a grain identification (GID) angle of 15° and thin lines 2° . Others were fragmented into small grains with high angle grain boundaries. Three cycles of ARB process shattered most initial grains and they were elongated severely. Grain refinement and elongation during ARB process were clear in five cycles.

Morphological features of AA1100 during ARB process were examined based on EBSD data presented in Fig. 1. Variations in grain size and aspect ratio (the ratio of the width of grains to their height) were examined in Fig. 2. They evolved in the opposite direction with increase in strain (or ARB pass). Initial grain size was about $20 \mu\text{m}$ and it continued to decrease down to $5 \mu\text{m}$. Conversely, aspect ratio increased with ARB pass. Initial aspect ratio of undeformed grains was about 1.5 and it increased up to 3.5 after 5 cycles.

Crystallographic texture evolution during ARB was also of interest. Figure 3 shows recalculated (111) PF (pole figure) and ODF (orientation distribution function, $\phi_2=45^\circ$ section). When computing PF and ODF from EBSD data, cubic crystal and orthorhombic sample systems were assumed. Initial texture revealed a strong Cube component and a weak β (Brass-S-Copper) fiber. The former is known as a typical recrystallization texture, and the latter is the rolling texture components of cubic metals. It is usual to find the recrystallized Cube component after recrystallization. It, however, is interesting to find some amount of rolling texture components remaining even after recrystallization. As seen in Fig. 1, microstructure displayed full recrystallization, and thus the remained deformation textures seem to be a part of continuous recrystallization or extended recovery. With increase in strain, overall texture components are α (Goss-Brass) and β fibers, which are developing under rolling or plane strain compression (PSC) conditions. The initial Cube component, which is unstable under PSC condition [10], decreased with strain. There existed some amount of the Goss component after 1 and 3 passes of ARB. Further strains of 5 passes revealed that most of texture components were the β fiber. For more detailed quantitative texture analysis, volume calculation of each texture components can be utilized [9]. Figure 4 presents volume fraction of each texture component during ARB. Texture volume of each component in the initial sheets implies that most dominant initial textures are close to homogeneous orientations or random texture excluding major recrystallization and deformation texture components. Major 6 components calculated had about 30

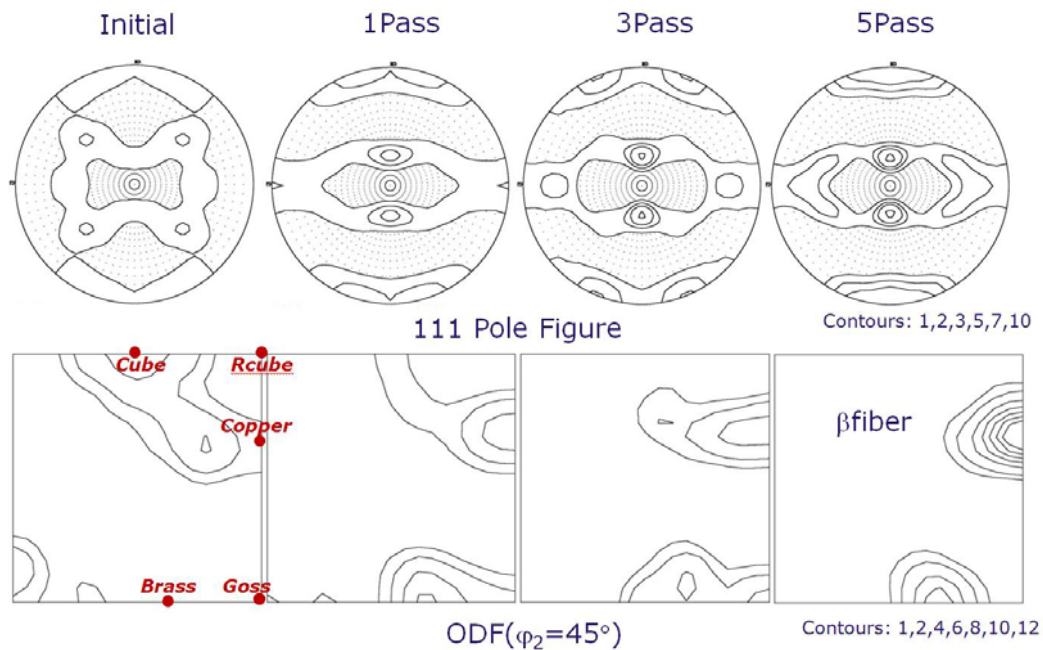


Fig. 3. Pole figure and ODF ($\varphi_2=45^\circ$ section) showing texture evolution during ARB.

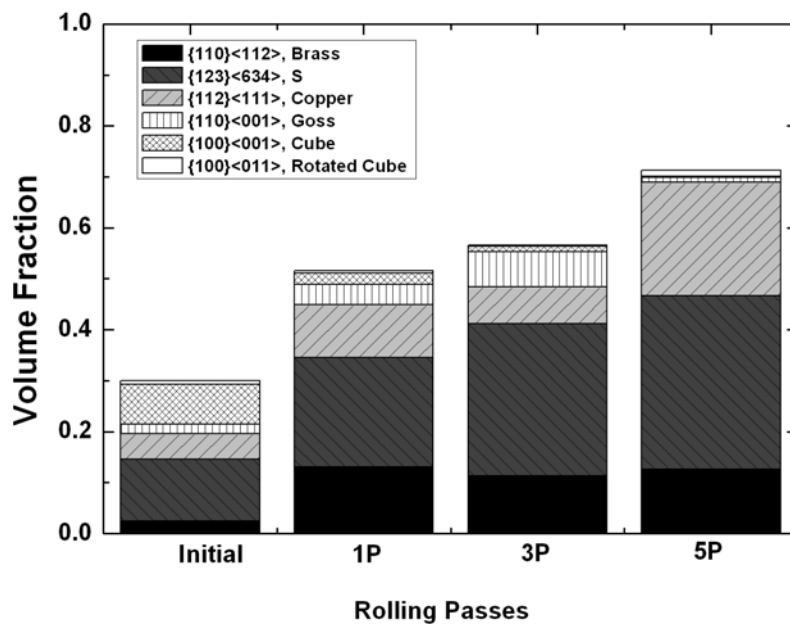


Fig. 4. Variations in texture volume fraction during ARB.

percent of the total volume fraction and the others 70 percent. It is evident that the β fiber increased with strain and reached almost 70 percent after 5 passes.

Scalar orientation spread (SOS) is one of the misorientation measures to characterize orientation gradient inside grains [11]. It was determined from EBSD data by considering accumulative misorientation angles between mean orientation and each pixel inside grains of interest. Misorientation inside grains tends to increase during deformation and sharply drops after

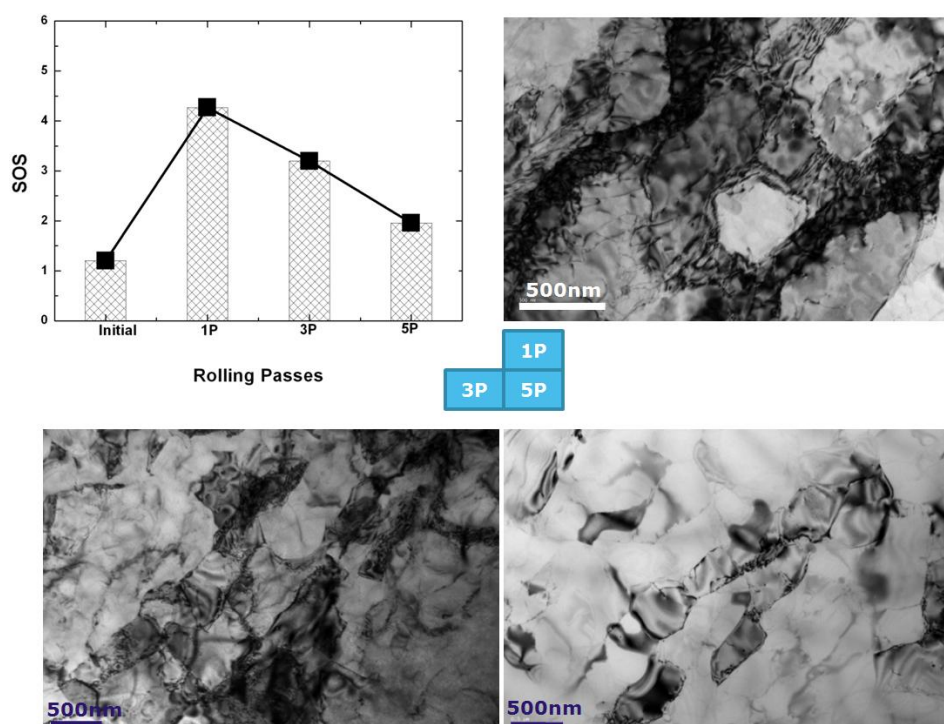


Fig. 5. SOS variations and TEM micrographs.

recrystallization. Higher SOS means that the grains have high dislocation density, or highly-deformed region with orientation gradient. The top-left graph in Figure 5 illustrates SOS. Initial sample shows the lowest value of SOS. After the first pass of ARB, most of grains were shattered and heavily-deformed, and this resulted in increased SOS. Three and five cycles of TRB processes gradually lowered SOS values. To further examine microstructural features of ARBed sheet, TEM micrographs are also presented. The TEM micrograph for the first pass revealed a great deal of dislocation tangles and cell boundaries. In the TEM micrograph after three cycles, cell boundaries or subgrain boundaries formed and high angle grain boundaries developed. After five cycles, high angle grain boundaries were clearer and few dislocations were found inside grains because of enhanced dynamic recovery or dynamic recrystallization.

4. Conclusions

Three layers of AA1100 sheets were bonded using ARB process. Texture and microstructure evolution during ARB was investigated using EBSD and TEM. With increase in strain, grain size decreased and aspect ratio increased. After five cycles, overall dimension of elongated grains had great aspect ratio with submicron width and micron length. TEM micrographs and misorientation measure of SOS revealed evolution of dislocation density with strain. In low strain, there existed original high angle grain boundaries with a lot of dislocation tangles inside. With increase in strain, dislocation cells and subgrain boundaries became into high angle grain boundaries, and few dislocations were found inside grains. Severe deformation resulted in increase in strength and decrease in elongation.

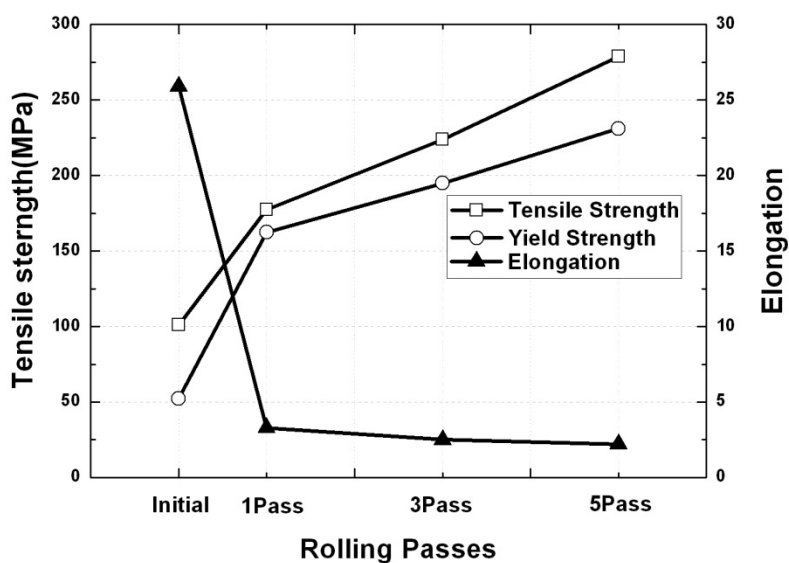


Fig. 6. Tensile strength and elongation.

Figure 6 shows tensile strength and elongation of ARBed sheets without annealing. Heavy deformation quickly reduced elongation, and gradually increased tensile and yield strengths.

References

- [1] F. J. Humphreys, P. B. Prangnell, and R. Priestner, *Current Opinion in Solid State and Mater. Sci.* 5 (2001) 15–21.
- [2] P.J. Apps, M. Berta, P.B. Prangnell, *Acta Materialia* 53 (2005) 499–511.
- [3] M. Janeček, M. Popov, M.G. Krieger, R.J. Hellmig, Y. Estrin, *Mater. Sci. and Eng. A* 462 (2007) 116–120.
- [4] Y. Saito, H. Utsunomiya, N. Tsuji and T. Sakai, *Acta mater.*, 47 (1999) 579-583.
- [5] S.H. Lee, Y. Saito, T. Sakai, H. Utsunomiya, *Mater. Sci. and Eng. A* 325 (2002) 228–235.
- [6] WANG Q. F. , XIAO X. P. li2, HU J. ' , XU W. W. ' , ZHAO X.Q. ' , ZHAO S. J. , *P. Sino-Swedish Struc. Mater. Symp.* 2007, 167-172.
- [7] K. Wu, H. Chang, E. Maawad, W.M. Gan, H.G. Brokmeier, M.Y. Zheng, *Materials Science and Engineering A* 527 (2010) 3073–3078.
- [8] L. Zaharia, R. Comaneci, C. Baciuc and N. Cimpoesu, *Proceedings of the 9th Biennial ASME conference on Engineering systems design and Analysis ESDA 2008-59234.*
- [9] J. H. Cho, A. D. Rollett, K. H. Oh, *Metal. Mater. Trans. A* 35 (2004) 1075-1086.
- [10] A. Kumar and R. R. Dawson, *Acta Mater.* 48 (2000) 2719-2736.
- [11] J. H. Cho, J. S. Cho, J.T. Moon, J. Lee, Y. H. Cho, Y.W. Kim, A.D. Rollett, and K.H. Oh, *Metal. Mater. Trans. A* 34 (2003) 1113-1125.